

Synthesis of Thiophene-Based π -Conjugated Polymers Containing Oxadiazole or Thiadiazole Moieties and Their Application to Organic Photovoltaics

Tomoya Higashihara,^{*,†,‡} Hung-Chin Wu,^{§,⊥} Tetsunari Mizobe,^{†,⊥} Chien Lu,[§] Mitsuru Ueda,[†] and Wen-Chang Chen^{*,§}

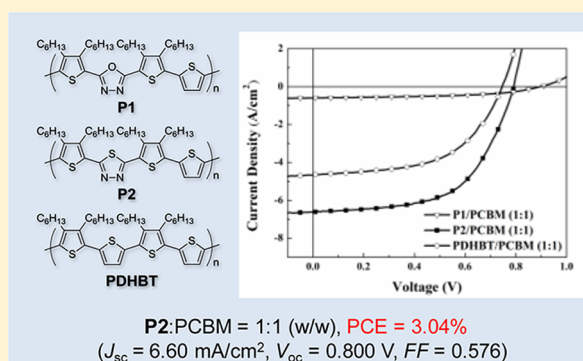
[†]Department of Organic and Polymeric Materials, Graduate School of Science and Engineering, Tokyo Institute of Technology, 2-12-1 O-okayama, Meguro-ku, Tokyo 152-8552, Japan

[‡]Japan Science and Technology Agency (JST), PRESTO, 4-1-8, Honcho, Kawaguchi, Saitama 332-0012, Japan

[§]Department of Chemical Engineering, National Taiwan University, Taipei, Taiwan 10617

Supporting Information

ABSTRACT: We report the synthesis, properties, and photovoltaic applications of new π -conjugated polymers having thiophene, 3,4-dihexylthiophene, and 1,3,4-oxadiazole (OXD) or 1,3,4-thiadiazole (TD) units in the main chain, denoted as **P1** and **P2**. They were synthesized by the Stille coupling reaction of 2,5-bis(trimethylstannyl)thiophene and the corresponding monomers of 2,5-bis(*S'*-bromo-3',4'-dihexylthien-2'-yl)-1,3,4-oxadiazole or 2,5-bis(*S'*-bromo-3',4'-dihexylthien-2'-yl)-1,3,4-thiadiazole, respectively. The experimental results indicated that the introduction of an electron-accepting moiety of OXD or TD lowered the highest occupied molecular orbital (HOMO) energy levels, resulting in the higher the open-circuit voltage (V_{oc}) values of polymer solar cells (PSCs). Indeed, the PSCs of **P1** and **P2** showed high V_{oc} values in the range 0.80–0.90 V. The highest field-effect transistor (FET) mobilities of **P1** and **P2** with the OXD and TD moieties, respectively, were 1.41×10^{-3} and $8.81 \times 10^{-2} \text{ cm}^2 \text{ V}^{-1} \text{ s}^{-1}$. The higher mobility of **P2** was related to its orderly nanofibrillar structure, as evidenced from the TEM images. Moreover, the higher absorption coefficient and smaller band gap of **P2** provided a more efficient light-harvesting ability. The power conversion efficiency (PCE) of the PSC based on **P2**:PCBM = 1:1 (w/w) reached 3.04% with a short-circuit current density (J_{sc}) value of 6.60 mA/cm², a V_{oc} value of 0.80 V, and a fill factor (FF) value of 0.576 during the illumination of AM 1.5, 100 mW/cm². In comparison, the parent PDHBT without the electron-accepting moiety exhibited an inferior device performance (FET mobility = $2.10 \times 10^{-4} \text{ cm}^2 \text{ V}^{-1} \text{ s}^{-1}$ and PCE = 1.91%). The experimental results demonstrated that incorporating the electron-acceptor moiety into the polythiophene backbone could enhance the device performance due to the low-lying HOMO levels, compact packing structure, and high charge carrier mobility. This is the first report for the achievement of PCE > 3% using PSCs based on polythiophenes having TD units in the main chain.



INTRODUCTION

Bulk-heterojunction (BHJ) polymer solar cells (PSCs), in which the photoactive layer consists of an interpenetrating network of a π -conjugated polymer donor (D) and a soluble fullerene acceptor (A), have attracted much attention because of their easy processability, low material costs, high efficiency, and mechanical flexibility.^{1–14} One of the most successful system until now utilizes a blend of regioregular poly(3-hexylthiophene) (P3HT) and [6,6]-phenyl-C₆₁-butyric acid methyl ester (PCBM) as the active layer, normally giving power conversion efficiencies (PCEs) in the range of 4–5%.^{2,6,7} However, the highest occupied molecular orbital (HOMO) energy level of P3HT is too high (ca. -4.76 eV^{15}) which limits the open-circuit voltage (V_{oc}) values of the PSCs to ca. 0.6 V. It is well-known that the modulation of the HOMO/lowest

unoccupied molecular orbital (LUMO) energy levels for the polymers is essential to realize a high V_{oc} value without sacrificing the broad light harvesting and efficient charge separation, which correspond to a J_{sc} value.¹⁶ Donor–acceptor (D–A) polymers are attractive as p-type materials for PSCs due to the facile tunability of the HOMO/LUMO energy levels by properly choosing the D and A moieties. Indeed, much effort has been made to achieve very high PCEs over 7% for the PSC devices.^{17–22}

1,3,4-Oxadiazole (OXD) and 1,3,4-thiadiazole (TD) are electron-deficient units containing two electron-withdrawing

Received: September 23, 2012

Revised: October 30, 2012

Published: November 12, 2012

imine groups (C=N) and can be used as A units. For instance, a structure similar to the benzothiadiazole units has frequently been utilized as an A unit in D–A polymers to achieve high PCEs.^{23–28} However, a few reports have described the PSCs using D–A type polymers bearing OXD and TD units,^{29,30} regardless of their electron-withdrawing nature, as well as more compact structures compared to the benzothiadiazole units, which would be preferable for more densely packed structures for the polymer films to induce a high charge mobility.

We now report the synthesis of new D–A type polythiophene derivatives carrying OXD or TD units, i.e., **P1** and **P2** (see Figure 1), based on the Stille coupling reaction of

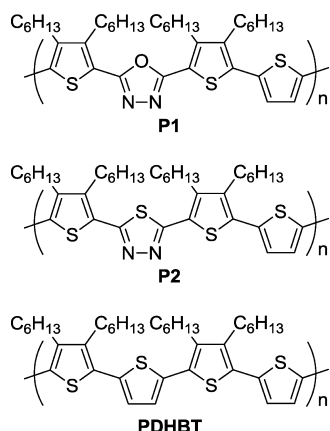


Figure 1. Chemical structures of **P1** and **P2**.

2,5-bis(trimethylstannyl)thiophene and the corresponding monomers of 2,5-bis(5'-bromo-3',4'-dihexylthien-2'-yl)-1,3,4-oxadiazole (**5**) or 2,5-bis(5'-bromo-3',4'-dihexylthien-2'-yl)-1,3,4-thiadiazole (**7**), respectively (see Scheme 1). The D–A polymers are soluble in common organic solvents and their chemical structures, molecular weight, thermal stability, optical and electronic properties, morphology, FET, and photovoltaic

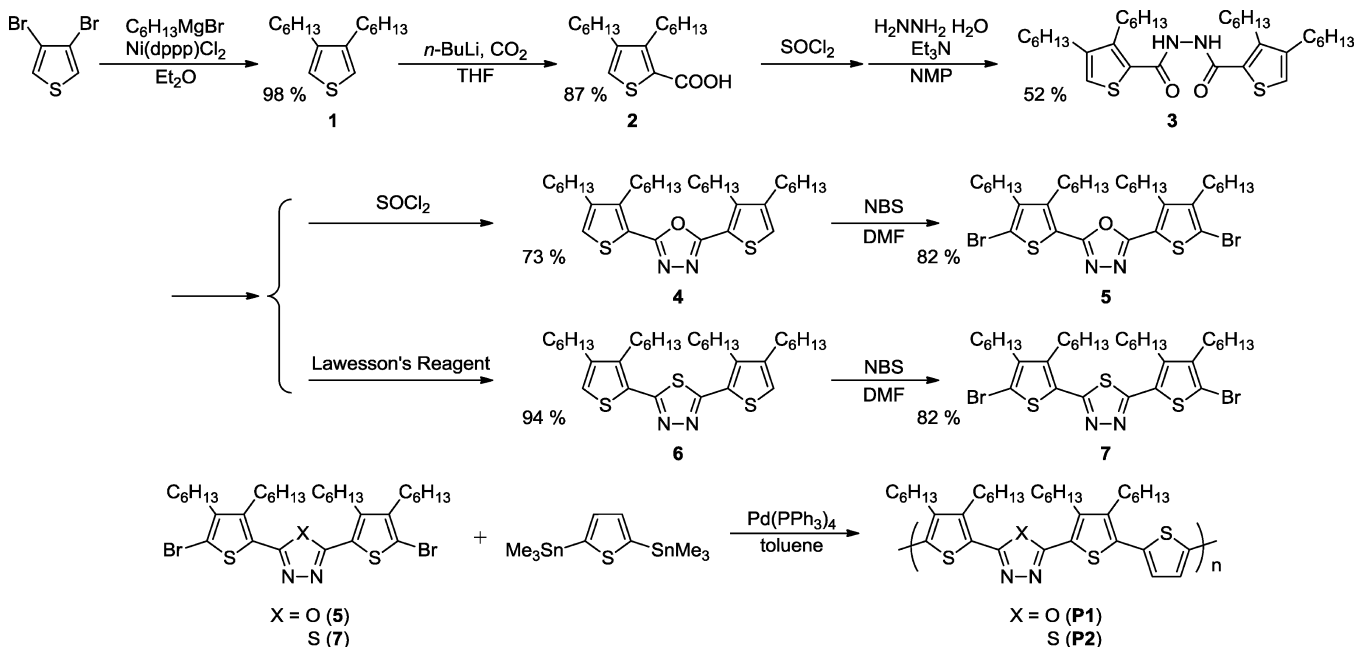
characteristics were fully investigated. The parent polymer, poly(3,4-dihexyl-2,2'-bithiophene) (PDHBT), without the OXD or TD moiety was prepared in order to compare the properties of **P1** and **P2**. In particular, **P1** and **P2** show HOMO levels of -5.55 and -5.33 eV, respectively, which are lower than that of PDHBT as expected. The BHJ PSC based on **P2**:PCBM = 1:1 (w/w) exhibits PCEs up to 3.04% with the high V_{oc} value of 0.80 V under the illumination of AM 1.5, 100 mW/cm², which is the first example of the TD-containing D–A polymers showing such a high PCE over 3%.

EXPERIMENTAL SECTION

Materials. Tetrahydrofuran (THF) was dried over sodium benzophenone and distilled before use under nitrogen. *N*-Methylpyrrolidone (NMP) and triethylamine were dried over calcium hydride and distilled before used under nitrogen. 3,4-Dihexylthiophene (**1**),³⁰ 2,5-bis(trimethylstannyl)thiophene,³¹ and PDHBT (SEC; $M_n = 12\,800$, PDI = 1.73)³² were prepared according to the literatures. All other reagents and solvents were used as received.

3,4-Dihexyl-2-thiophenecarboxylic Acid (2). To a THF solution (40 mL) of **1** (4.22 g, 16.7 mmol) was added dropwise at 0 °C a *n*-BuLi solution in hexane (2.67 M \times 6.90 mL = 18.4 mmol). The solution was then stirred for 1 h. After cooling the solution to -78 °C, it was poured onto dry ice in a beaker and stirred for 2 h. After the solution was warmed to room temperature, the reaction was then quenched with water and the product was extracted with ether. The ethereal solution was neutralized with HCl(aq) and then washed with water. After drying the solution over MgSO₄ followed by filtration, the filtrate was evaporated under the reduced pressure. The crude product was purified by flash silica gel column chromatography using hexane/ethyl acetate (9/1, v/v) as an eluent to afford **2** as yellow oil (4.30 g, 87%). ¹H NMR (300 MHz, CDCl₃, δ , ppm, 25 °C): 7.19 (s, 1H), 2.93 (t, 2H), 2.53 (t, 2H), 1.23–1.69 (m, 16H), 0.90 (t, 6H). ¹³C NMR (75 MHz, CDCl₃, δ , ppm, 25 °C): 167.5, 150.9, 143.3, 126.6, 125.2, 30.7, 30.6, 29.3, 28.7, 28.6, 28.1, 27.7, 26.8, 21.6, 13.1. IR, ν (cm⁻¹): 1666 (C=O stretching), 1446 (C–O–H bending), 1277 (C–O stretching). Anal. Calcd for C₁₇H₂₈O₂S (%): C, 68.87; H, 9.52. Found (%): C, 69.18; H, 9.36. MS m/z : Calcd for C₁₇H₂₇NaO₂S, 318.16; found, 318.27.

Scheme 1. Synthetic Routes for **P1** and **P2**



***N,N'*-Bis(3,4-dihexylthien-2-ylcarbonyl)hydrazine (3).** The thionyl chloride solution (6 mL) of **2** (4.05 g, 13.7 mmol) was refluxed for 2 h. After removing excess thionyl chloride under the reduced pressure, NMP (25 mL) and triethylamine (3 mL) were added. To this solution, hydrazine monohydrate (0.285 mL, 5.75 mmol) was added dropwise, and the solution was stirred overnight. It was then poured into water to precipitate the crude product. Flash silica gel column chromatography of the product using hexane/ethyl acetate (9/1, v/v) and recrystallization from ethanol/water afforded **3** as a white solid (2.08 g, 52%). T_m : 75–76 °C. $^1\text{H NMR}$ (300 MHz, CDCl_3 , δ , ppm, 25 °C): 8.58 (s, 2H), 7.02 (s, 2H), 2.88 (t, 4H), 2.52 (t, 4H), 1.22–1.68 (m, 32H), 0.90 (m, 12H). $^{13}\text{C NMR}$ (75 MHz, CDCl_3 , δ , ppm, 25 °C): 160.7, 148.5, 144.5, 126.7, 123.2, 31.8, 30.8, 29.9, 29.8, 29.3, 28.9, 28.1, 22.8, 14.2. IR, ν (cm^{-1}): 3190 (N–H stretching), 1651 (C=O stretching). Anal. Calcd for $\text{C}_{34}\text{H}_{56}\text{N}_2\text{O}_2\text{S}_2$ (%): C, 69.34; H, 9.58; N, 4.76. Found (%): C, 69.11; H, 9.26; N, 4.74. MS m/z : Calcd for $\text{C}_{34}\text{H}_{56}\text{N}_2\text{O}_2\text{S}_2$, 588.38; found, 588.27.

2,5-Bis(3',4'-dihexylthien-2'-yl)-1,3,4-oxadiazole (4). The thionyl chloride solution (5 mL) of **3** (0.738 g, 1.25 mmol) was heated at 70 °C for 30 min. After removing excess thionyl chloride under the reduced pressure, the crude product was obtained. It was then purified by flash silica gel (treated with triethylamine) column chromatography using hexane to afford **4** as yellow oil (0.525 g, 73%). $^1\text{H NMR}$ (300 MHz, CDCl_3 , δ , ppm, 25 °C): 7.11 (s, 2H), 3.01 (t, 4H), 2.57 (t, 4H), 1.22–1.73 (m, 32H), 0.90 (m, 12H). $^{13}\text{C NMR}$ (75 MHz, CDCl_3 , δ , ppm, 25 °C): 160.2, 146.2, 144.2, 124.1, 119.4, 31.7, 30.1, 29.7, 29.6, 29.2, 28.8, 28.2, 22.7, 22.6, 14.1. IR, ν (cm^{-1}): 1562 (C=N stretching). Anal. Calcd for $\text{C}_{34}\text{H}_{54}\text{N}_2\text{O}_2\text{S}_2$ (%): C, 71.53; H, 9.53; N, 4.91. Found (%): C, 72.13; H, 9.56; N, 5.43. MS m/z : Calcd for $\text{C}_{34}\text{H}_{54}\text{N}_2\text{O}_2\text{S}_2$, 570.37; found, 570.38.

2,5-Bis(5'-bromo-3',4'-dihexylthien-2'-yl)-1,3,4-oxadiazole (5). To **4** (0.508 g, 0.890 mmol) in DMF (5 mL) was added *N*-bromosuccinimide (NBS) (0.412 g, 2.31 mmol), and the solution was stirred overnight. The reaction was quenched with water, and the product was extracted with ether. After drying the ethereal solution over MgSO_4 followed by filtration, the filtrate was condensed under the reduced pressure. The crude product was then purified by flash silica gel (treated with triethylamine) column chromatography using hexane as an eluent to afford **5** as yellow oil (0.532 g, 82%). $^1\text{H NMR}$ (300 MHz, CDCl_3 , δ , ppm, 25 °C): 3.00 (t, 4H), 2.59 (t, 4H), 1.24–1.64 (m, 32H), 0.90 (m, 12H). $^{13}\text{C NMR}$ (75 MHz, CDCl_3 , δ , ppm, 25 °C): 159.5, 146.5, 143.7, 119.4, 114.9, 31.8, 31.7, 30.5, 29.8, 29.6, 29.4, 29.3, 28.6, 22.8, 14.3, 14.2. IR, ν (cm^{-1}): 1564 (C=N stretching). Anal. Calcd for $\text{C}_{34}\text{H}_{52}\text{Br}_2\text{N}_2\text{O}_2\text{S}_2$ (%): C, 56.04; H, 7.19; N, 3.84. Found (%): C, 56.73; H, 6.96; N, 3.82. MS m/z : Calcd for $\text{C}_{34}\text{H}_{52}\text{Br}_2\text{N}_2\text{O}_2\text{S}_2$, 728.19; found, 728.09.

2,5-Bis(3',4'-dihexylthien-2'-yl)-1,3,4-thiadiazole (6). A toluene solution (15 mL) of **3** (1.00 g, 1.70 mmol) and 2,4-bis(4-methoxyphenyl)-1,3,2,4-dithiadiphosphetane-2,4-dithione (Lawesson's reagent, 0.839 g, 2.08 mmol) was refluxed for 2 days. After removing toluene under the reduced pressure, the crude product was obtained. It was then purified by flash silica gel (treated with triethylamine) column chromatography using hexane as an eluent to afford **6** as yellow oil (0.933 g, 94%). $^1\text{H NMR}$ (300 MHz, CDCl_3 , δ , ppm, 25 °C): 7.07 (s, 2H), 2.89 (t, 4H), 2.56 (t, 4H), 1.22–1.72 (m, 32H), 0.90 (m, 12H). $^{13}\text{C NMR}$ (75 MHz, CDCl_3 , δ , ppm, 25 °C): 160.4, 144.0, 143.6, 127.0, 123.5, 31.7, 31.6, 29.9, 29.7, 29.2, 29.0, 28.5, 22.6, 14.1. IR, ν (cm^{-1}): 1551 (C=N stretching). Anal. Calcd for $\text{C}_{34}\text{H}_{54}\text{N}_2\text{S}_3$ (%): C, 69.57; H, 9.27; N, 4.77. Found (%): C, 70.15; H, 9.27; N, 5.29. MS m/z : Calcd for $\text{C}_{34}\text{H}_{54}\text{N}_2\text{S}_3$, 586.34; found, 586.27.

2,5-Bis(5'-bromo-3',4'-dihexylthien-2'-yl)-1,3,4-thiadiazole (7). To **6** (0.838 g, 1.43 mmol) in DMF (10 mL) was added NBS (0.889 g, 4.99 mmol), and the solution was stirred overnight. The reaction was quenched with water, and the product was extracted with ether. After drying the ethereal solution over MgSO_4 followed by filtration, the filtrate was condensed under the reduced pressure. The crude product was then purified by flash silica gel (treated with triethylamine) column chromatography using hexane as an eluent to afford **7** as yellow oil (0.875 g, 82%). $^1\text{H NMR}$ (300 MHz, CDCl_3 , δ ,

ppm, 25 °C): 2.86 (t, 4H), 2.58 (t, 4H), 1.24–1.62 (m, 32H), 0.91 (m, 12H). $^{13}\text{C NMR}$ (75 MHz, CDCl_3 , δ , ppm, 25 °C): 159.3, 143.4, 143.1, 127.1, 114.4, 31.5, 30.1, 29.7, 29.6, 29.4, 29.3, 28.5, 22.6, 14.1. IR, ν (cm^{-1}): 1549 (C=N stretching). Anal. Calcd for $\text{C}_{34}\text{H}_{52}\text{Br}_2\text{N}_2\text{S}_3$ (%): C, 54.83; H, 7.04; N, 3.76. Found (%): C, 55.18; H, 6.79; N, 4.09. MS m/z : Calcd for $\text{C}_{34}\text{H}_{52}\text{Br}_2\text{N}_2\text{S}_3$, 744.16; found, 743.97.

Poly[2,5-thiophene-*alt*-5',5'-(2'',5'')-bis(3',4'-dihexylthien-2'-yl)-1'',3'',4''-oxadiazole] (P1). To **5** (0.399 g, 0.548 mmol) and 2,5-bis(trimethylstannyl)thiophene (0.225 g, 0.548 mmol) was added $\text{Pd}(\text{PPh}_3)_4$ (6.0 mg, 0.005 mmol) in toluene (15 mL) in argon, which was deoxidized by bobbling with dry argon for 15 min. The solution was refluxed for 2 days. After quenching the reaction with $\text{HCl}(\text{aq})$ and neutralizing with $\text{NaHCO}_3(\text{aq})$, the product was extracted with CHCl_3 . The CHCl_3 solution was then washed with $\text{KF}(\text{aq})$. CHCl_3 was removed under the reduced pressure, and THF was added. The THF solution was poured into water to precipitate the polymer. The polymer was purified by Soxhlet extraction using methanol, acetone, acetone/hexane (1/1, v/v), and CHCl_3 . After evaporating CHCl_3 , the polymer was further purified by flash silica gel column chromatography using CHCl_3 as an eluent, followed by freeze-drying from its absolute benzene solution, to afford **P1** as orange solid (0.185 g, 52%). SEC: $M_n = 18\,500$; PDI = 1.45. $^1\text{H NMR}$ (300 MHz, CDCl_3 , δ , ppm, 25 °C): 7.22 (s, 2H), 3.05 (s, 4H), 2.81 (s, 4H), 1.21–1.74 (m, 32H), 0.91 (m, 12H). IR, ν (cm^{-1}): 1562 (C=N stretching).

Poly[2,5-thiophene-*alt*-5',5'-(2'',5'')-bis(3',4'-dihexylthien-2'-yl)-1'',3'',4''-thiadiazole] (P2). To **7** (0.326 g, 0.438 mmol) and 2,5-bis(trimethylstannyl)thiophene (0.179 g, 0.438 mmol) was added $\text{Pd}(\text{PPh}_3)_4$ (5.3 mg, 0.005 mmol) in toluene (15 mL) in nitrogen, which was deoxidized by bobbling with dry nitrogen for 15 min. The solution was refluxed for 2 days. After quenching the reaction with $\text{HCl}(\text{aq})$ and neutralizing with $\text{NaHCO}_3(\text{aq})$, the product was extracted with CHCl_3 . The CHCl_3 solution was then washed with $\text{KF}(\text{aq})$. The CHCl_3 solution was condensed under the reduced pressure and poured into water/methanol to precipitate the polymer. The polymer was purified by Soxhlet extraction using methanol, acetone, hexane, and CHCl_3 . After evaporating CHCl_3 , the polymer was further purified by flash silica gel column chromatography using CHCl_3 as an eluent, followed by freeze-drying from its absolute benzene solution, to afford **P2** as red solid (0.226 g, 77%). SEC: $M_n = 24\,400$; PDI = 1.88. $^1\text{H NMR}$ (300 MHz, CDCl_3 , δ , ppm, 25 °C): 7.23 (s, 2H), 2.92 (s, 4H), 2.80 (s, 4H), 1.20–1.73 (m, 32H), 0.92 (m, 12H). IR, ν (cm^{-1}): 1551 (C=N stretching).

Fabrication and Characterization of Field-Effect Transistors (FET). Highly doped n-type Si(100) wafers were used as substrates. A 300 nm SiO_2 layer (capacitance per unit area $C_0 = 10 \text{ nF cm}^{-2}$) as a gate dielectric was thermally grown onto the Si substrates. These wafers were cleaned in piranha solution, a 7:3 (v/v) mixture of H_2SO_4 and H_2O_2 , rinsed with deionized water, and then dried by nitrogen. The octadecyltrichlorosilane (ODTS)-treated surfaces on SiO_2/Si substrates were obtained by the following procedure: a clean SiO_2/Si substrate was immersed into a 10 mM solution of trichlorosilane in toluene at 80 °C for 2 h. Then the substrates were rinsed with toluene and dried with a stream of nitrogen. FET devices were deposited by spin-coating from chlorobenzene (10–12 mg/mL) at a spin rate of 800 rpm for 60 s and annealing at 100 °C for 60 min. The top-contact source and drain electrodes were defined by 100 nm thick gold through a regular shadow mask, and the channel length (L) and width (W) were 50 and 1000 μm , respectively. FET transfer and output characteristics were recorded in a nitrogen-filled glovebox by using a Keithley 4200 semiconductor parametric analyzer.

Fabrication and Characterization of Polymer Solar Cells. All the BHJ PSCs were prepared using the same preparation procedures and device fabrication procedure referring as follows: The glass-indium tin oxide (ITO) substrates (obtained from Lumtec, Ltd. (7 Ω/sq)) were first patterned by lithograph, then cleaned with detergent, ultrasonicated in acetone and isopropyl alcohol, subsequently dried on a hot plate at 120 °C for 5 min, and finally treated with oxygen plasma for 5 min. Poly(3,4-ethylenedioxythiophene):poly(styrenesulfonate) (PEDOT:PSS, Baytron P VP AI4083) was passed through a 0.45 μm filter before being deposited on ITO with a thickness around 30 nm by

spin-coating at 5000 rpm in the air and dried at 140 °C for 20 min inside a glovebox. The blended film of the polymer/PCBM (1:1, by wt) was prepared by dissolving them in anhydrous chlorobenzene (8–12 mg/mL) followed by spin-coating on the top of PEDOT:PSS layer at the speed rate of 600–800 rpm for 50 s. Subsequently, the devices were completed by thermal evaporation of Ca (30 nm) and Al (100 nm) under high-vacuum condition ($<10^{-6}$ Torr). The active area of the device is 4 mm². The current density–voltage (J – V) measurement of the PSC was conducted by a computer-controlled Keithley 2400 source measurement unit (SMU) with a Peccell solar simulator under the illumination of AM 1.5G, 100 mW/cm². The illumination intensity was calibrated by a standard Si photodiode detector with KG-5 filter, and no additional mask was used under the illumination.

Measurements and Characterization. Molecular weights (MWs) and polydispersity indices (PDIs) were measured by SEC on a Jasco GULLIVER 1500 equipped with a pump, an absorbance detector (UV, $\lambda = 254$ nm), and three polystyrene gel columns based on a conventional calibration curve using polystyrene standards. CHCl₃ (40 °C) was used as a carrier solvent at a flow rate of 1.0 mL/min. ¹H and ¹³C NMR spectra were recorded on a Bruker DPX (300 MHz) in chloroform-*d* calibrated to tetramethylsilane as an internal standard (δ_{H} 0.00). FT-IR spectra were measured on a Horiba FT-720 spectrometer. Matrix-assisted laser desorption ionization time-of-flight (MALDI-TOF) mass spectra were recorded on a Shimadzu AXMA-CFR mass spectrometer. The spectrometer was equipped with a nitrogen laser (337 nm) and with pulsed ion extraction. The operation was performed at an accelerating potential of 20 kV by linear-positive ion mode. Dithranol was used as a matrix. Mass values were calibrated by the three-point method with insulin plus H⁺ at m/z 5734.62, insulin β plus H⁺ at m/z 3497.96, and α -cyanohydroxycinnamic acid dimer plus H⁺ at m/z 379.35. Thermal analysis was performed on a Seiko EXSTAR 6000 TG/DTA 6300 thermal analyzer at a heating rate of 10 °C/min for thermogravimetry (TG) and a TA Instruments Q-100 connected to a cooling system at a heating rate of 10 °C min⁻¹ for differential scanning calorimetry (DSC). UV–vis absorption spectra were recorded using a Hitachi U-4100 spectrophotometer. For the thin film spectra, polymers were first dissolved in chlorobenzene, followed with filtering through a 0.45 μm pore size PTFE membrane syringe filter, and then spin-coated at a speed rate of 800 rpm for 60 s onto quartz substrate. The absorption coefficients (α) were calculated by Beer's law, and the film thickness was determined with a Microfigure Measuring Instrument (Surfcorder ET3000, Kosaka Laboratory Ltd.). CV was performed with the use of a three-electrode cell in which ITO was used as a working electrode, and the polymer film was coated on it in 0.5×0.7 cm². A platinum wire was used as an auxiliary electrode. All cell potentials were taken in a 0.1 mol/L acetonitrile solution of tetrabutylammonium perchlorate at a scan rate of 0.1 V/s with the use of a homemade Ag/AgCl, KCl(sat.) reference electrode. The measurements of grazing-incidence wide-angle X-ray diffraction (GIXD) were performed with a Nano-Viewer (Rigaku) using Cu $K\alpha$ X-rays (30 kV and 40 mA) with wavelength $\lambda = 1.54$ Å and exposure durations of 30 min for each data correction. 2-Dimensional GIXD patterns were collected with Fuji plates at incidence angle 0.2°, which is an optimal angle less than the critical angles of samples and substrates. 1-Dimensional out-of-plane profiles with intensity as a function of 2θ were displayed upon scan cuts on the 2D GIXD patterns after instrumental calibrations. Transmission electron microscopy (TEM) was performed using a JEOL 1230 operated at an acceleration voltage of 100 kV. AFM measurements were obtained with a NanoScope IIIa AFM (Digital Instruments, Santa Barbara, CA) at room temperature. Commercial silicon cantilevers (Nanosensors, Germany) with typical spring constants of 21–78 N/m was used to operate the AFM in tapping mode. Images were taken continuously with the scan rate of 1.0 Hz.

Computational Methodology. Theoretical molecular simulations of the studied copolymers were calculated through the Gaussian 03 program package.³⁴ The density functional theory (DFT) method, using Becke's three-parameter functional with the Lee, Yang, and Parr correlation functional method (B3LYP) with 6-31G(d), was exploited for the optimized molecular geometry.

RESULTS AND DISCUSSION

Synthesis of Polymers. The general synthetic strategy for the monomers and polymers is outlined in Scheme 1. The alternative D–A type copolymers, **P1** and **P2**, were synthesized by the Stille coupling reaction of 2,5-bis(trimethylstannyl)-thiophene with **5** or **7**, respectively. Since a decrease in the solubility was expected by introducing the unsubstituted five-membered ring of OXD and TD, the 3,4-dihexylthiophene units were incorporated. As a result, **P1** and **P2** were quite soluble in the common organic solvents such as THF, CHCl₃, benzene, toluene, chlorobenzene, and *o*-dichlorobenzene. The number-average molecular weights and polydispersity indices (M_n , PDI) of **P1** and **P2** determined by SEC in CHCl₃ with a calibration using polystyrene standards are (18 500, 1.45) and (24 400, 1.88), respectively, as listed in Table 1. The results

Table 1. Molecular Weights and Thermal Properties of the Polymers

polymers	M_n^a	PDI ^a	T_d (°C) ^b	T_m (°C) ^c	T_c (°C) ^c
P1	18 500	1.45	403	174	140
P2	24 400	1.88	393	217	197

^a M_n and PDI of the polymers were determined by SEC using polystyrene standards in CHCl₃. ^bThe 5% weight-loss temperatures under an inert atmosphere. ^cThe T_m and T_c values were determined by DSC.

indicated that **P1** and **P2** possess adequate molecular weights. The SEC curves of **P1** and **P2** are shown in Figure S1 of the Supporting Information. Figure 2 shows the ¹H NMR spectra of **P1** and **P2**. In both cases, characteristic signals appear assignable to the 3- and 4-protons of the unsubstituted thiophene ring at 7.22 ppm (**P1**) and at 7.23 ppm (**P2**). In addition, the signals assignable to the methylene protons next to the thiophene ring can also be seen at 3.05 and 2.81 ppm (**P1**) and at 2.92 and 2.80 ppm (**P2**), the intensities of which are reasonably compared to the ones of the signals for the 3- and 4-protons of the unsubstituted thiophene ring. Thus, the above results suggest the successful synthesis of the target polymers.

The thermal stability of the two polymers was investigated by TGA, as shown in Figure S2. The onset decomposition temperatures of **P1** and **P2** for a 5% weight loss are 403 and 393 °C, respectively (see also Table 1), indicating that the thermal stability of the two polymers is sufficient for application in optoelectronic devices.

Optical and Electrochemical Properties. The UV–vis absorption spectra of the polymers in chlorobenzene are depicted in Figure 3a, which show the maximum absorption wavelength (λ_{max}) at 423 nm (**P1**), 467 nm (**P2**), and 446 nm (PDHBT), respectively. In the film states, the λ_{max} values of both polymers bathochromically shift to 470 nm (**P1**), 513 nm (**P2**), and 510 nm (PDHBT), respectively, indicating the structure ordering in these films (see Figure 3b). **P1** has the λ_{max} value in the wavelength region shorter than **P2** because of less crystalline nature, as will be described later. In addition, **P1** has a lower λ_{max} value than PDHBT. From the Gaussian simulation (Figure S3), the studied polymers show almost planar structures, which the torsional angles are generally smaller than 1.5°. The result indicates there is no obvious steric hindrance to affect energy band gaps. Hence, **P2** and PDHBT have smaller band gap than **P1**, probably due to the sulfur element having a larger atomic radius, more effectively

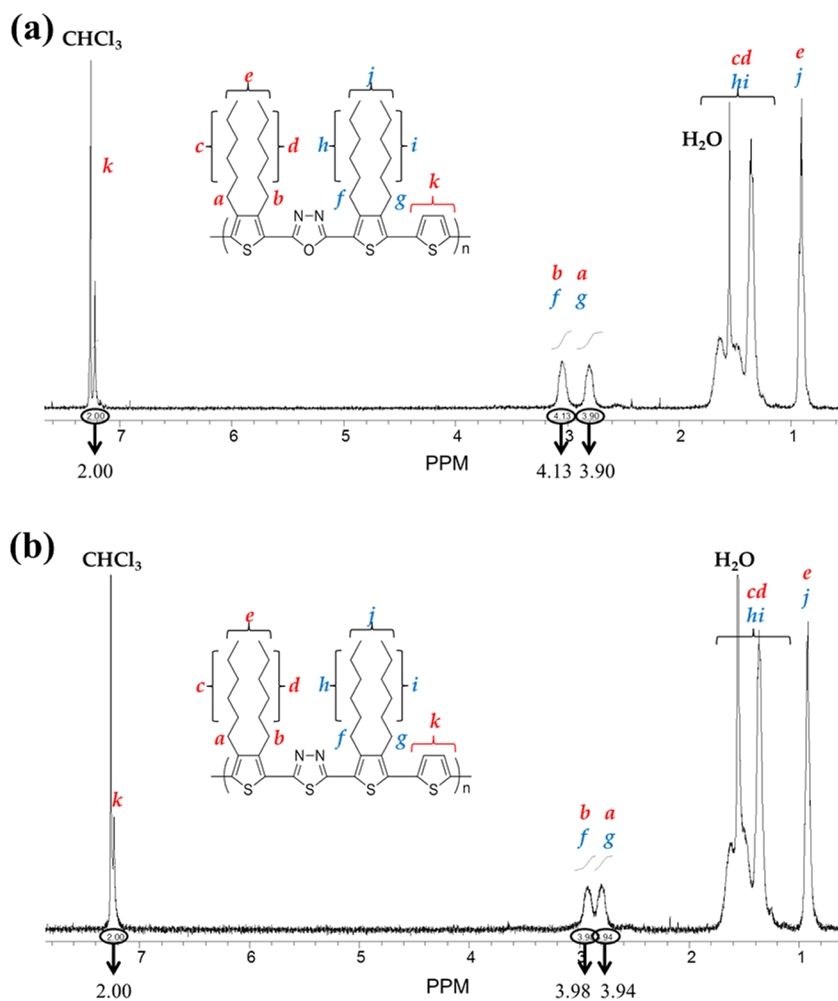


Figure 2. ^1H NMR spectra of (a) P1 and (b) P2 in CDCl_3 .

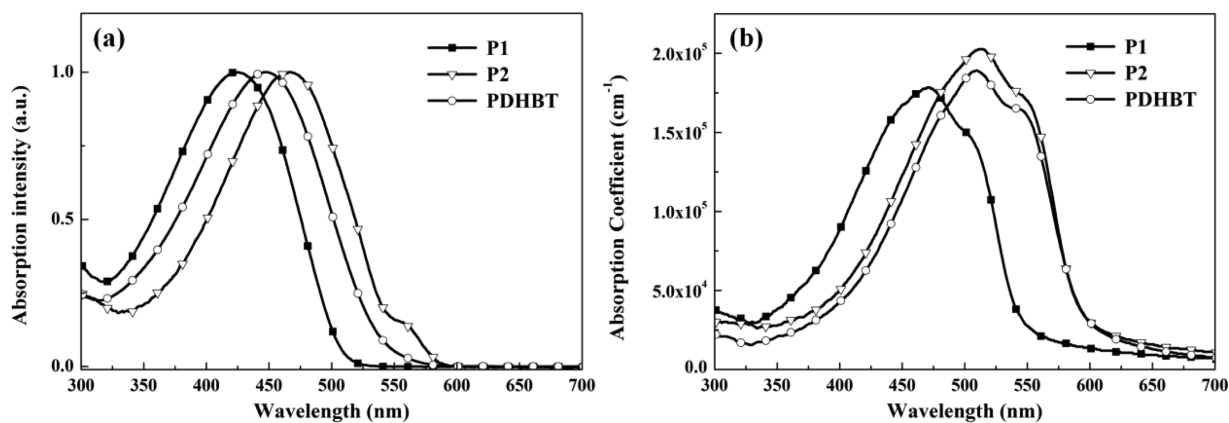


Figure 3. Optical absorption spectra of P1, P2, and PDHBT (a) in dilute chlorobenzene solutions and (b) in solid films on quartz plates.

hybridizing s and p orbitals, and being more polarizable, which are favorable for intermolecular interactions in thin films.³⁵ The calculated optical band gap (E_g^{opt}) values of P1 and P2 from the onset wavelengths of 542 nm (P1, film state) and 591 nm (P2, film state) are 2.29 and 2.10 eV, respectively. These results are summarized in Table 2, and they indicate that P2 absorbs light more efficiently compared to P1, which would be more preferable for the PSC performance.

Furthermore, the absorption coefficients of the thin films of P1 ($1.78 \times 10^5 \text{ cm}^{-1}$ at ca. 470 nm), P2 ($2.03 \times 10^5 \text{ cm}^{-1}$ at ca.

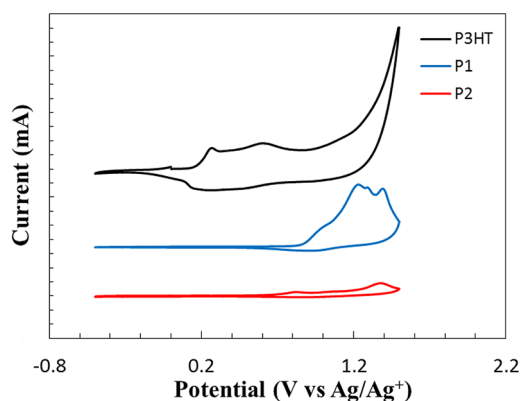
513 nm), and PDHBT ($1.89 \times 10^5 \text{ cm}^{-1}$ at ca. 510 nm) are comparable to that of the P3HT film ($1.9 \times 10^5 \text{ cm}^{-1}$ at ca. 552 nm).³⁶ Also, by incorporating the TD electron acceptor into polymer main chain, P2 shows a higher absorption coefficient than PDHBT. The high absorption coefficient of P2 suggests its potential to enhance the PSC characteristics.

The electrochemical CV (Figure 4) of P1 and P2 was performed in acetonitrile at a potential scan rate of 0.1 V/s for determining their HOMO energy levels. The CV curves of the P1 and P2 films show the oxidation peaks with the onset

Table 2. Optical Properties and Energy Levels of P1, P2, and PDHBT

polymers	λ_{\max}^a (nm)		α^b ($\times 10^5 \text{ cm}^{-1}$)	$E_g^{\text{opt}c}$	HOMO ^d (eV)	LUMO ^e (eV)
	solution	film				
P1	423	470	1.78	2.29	-5.55	-3.26
P2	467	513	2.03	2.10	-5.33	-3.23
PDHBT	446	510	1.89	2.11	-5.22 ³³	-3.12

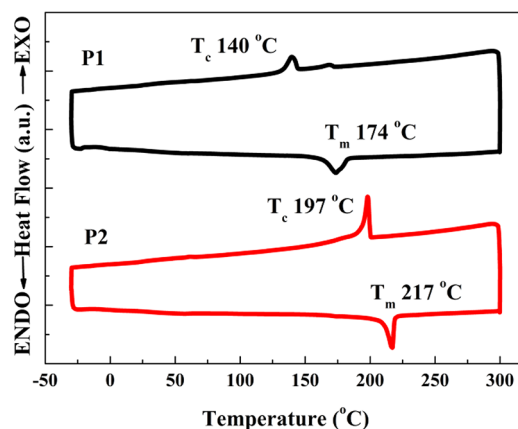
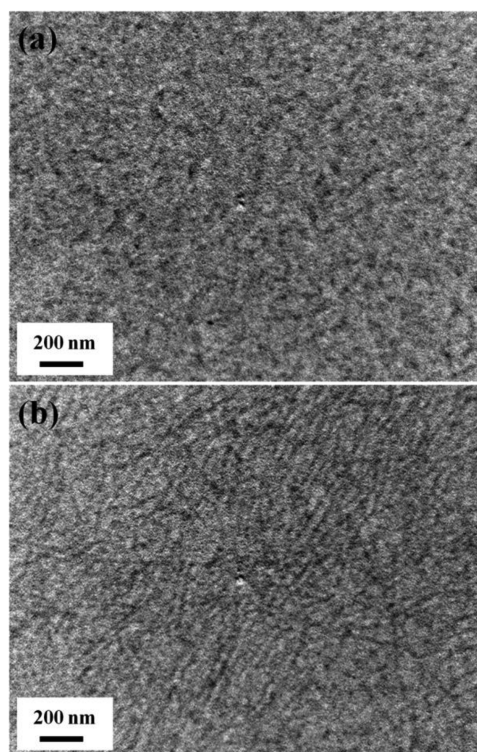
^aAbsorption maxima. ^bAbsorption coefficient (α) of the solid thin film at its maximum peak intensity in the visible region (420–700 nm) ($\times 10^{-5} \text{ cm}^{-1}$). ^cOptical band gap estimated from the onset of absorption spectra in solid film. ^dDetermined from the onset oxidation based on the reference energy level (ref 37). ^eCalculated by the equation $\text{LUMO} = \text{HOMO} + E_g^{\text{opt}}$ (eV).

**Figure 4.** Cyclic voltammograms of P3HT, P1, and P2 films on an ITO electrode in 0.1 mol/L tetrabutylammonium perchlorate CH_3CN solutions at a scan rate of 0.1 V/s.

oxidation potentials (φ_{ox}) of 0.866 and 0.646 V versus Ag/Ag^+ , corresponding to the HOMO energy level of -5.55 and -5.33 eV, respectively (Figure 4). Note that the HOMO energy level is estimated using the following relation: $\text{HOMO} = -e(E^{\text{ox}}(\text{onset}) - E^{1/2}(\text{ferrocene}) + 4.8)$ (eV).³⁷ It was found that both polymers possess lower HOMO energy levels than P3HT (-4.88 eV as measured under the same conditions) and PDHBT (-5.22 eV³²), which should be consistent with the high V_{oc} values from the PSC characterization, as described below. The LUMO energy levels of P1 and P2 were determined to be -3.26 and -3.23 eV, respectively, by the calculation of $\text{LUMO} = \text{HOMO} + E_g^{\text{opt}}$. All the CV data are also summarized in Table 2.

Morphological Characterization. DSC was used to investigate the possible crystallization of the prepared polymers. As shown in Figure 5, there are distinct endothermic peaks for the T_m values at 174 °C (P1) and 217 °C (P2) and corresponding exothermic peaks for the T_c values at 140 °C (P1) and 197 °C (P2), respectively, as listed in Table 1. It is obvious that P2 exhibits more distinct transition peaks than P1, which may be caused by highly ordered packing structures. These data are summarized in Table 1.

Figure 6 shows the TEM images of the thermally annealed P1 and P2 thin films. The annealed P2 thin film shows a distinct organized nanofibrillar structure as compared to P1. The well-ordered nanofibrillar morphology of P2 could result in good charge carrier transporting characteristics. The GIXD analyses of the P1 and P2 thin films (thickness of 40–50 nm) were carried out to further investigate their structural ordering,

**Figure 5.** DSC thermograms of P1 and P2 at the heating rate of 10 °C min^{-1} under a nitrogen atmosphere.**Figure 6.** TEM images of (a) P1 and (b) P2 films prepared from chlorobenzene solutions and annealed at 100 °C for 60 min.

as shown in Figure 7. Although the P1 film without annealing does not show a distinct diffraction peak except for the amorphous halo around $2\theta = 21^\circ$, a new diffraction peak appeared at $2\theta = 4.6^\circ$, corresponding to the d_1 spacing value of 19.2 Å after annealing at 100 °C. In contrast, the P2 film exhibited a distinct diffraction peak at $2\theta = 4.3^\circ$, corresponding to the d_1 spacing value of 20.5 Å without annealing. In addition, after annealing at 100 °C, the d_1 spacing value decreased to 18.4 Å, indicating more compact packing structures. Moreover, as compared to PDHBT (Figure S4), the studied polymers exhibit the smaller d_1 spacing (P1 (19.2 Å) and P2 (18.4 Å)) than PDHBT (24.5 Å) after annealing. This result may be due to the acceptor moieties incorporated into the polymer backbone that enhances the D–A intramolecular charge transfer. All the results supported the fact that P2 shows the highest degree of crystalline nature, which well agrees with the optical property

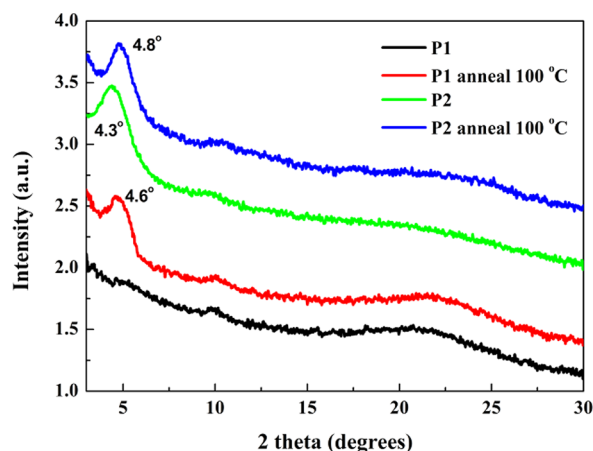


Figure 7. Out-of-plane GIXD profiles of **P1** and **P2** films prepared by spin-coating on the ODTs-treated substrates from chlorobenzene solutions.

observed from the optical absorption and thermal property. Besides, the nanofibrillar morphology of **P2** is also observed in the tapping mode AFM phase images (Figure S5). The ordered nanofibrillar structure of the **P2** film with the interconnected networks of the polymer chains may allow the formation of highly efficient pathways for charge carrier transport.^{38,39}

Field Effect Transistor (FET) Characteristics. Solution-processed FETs based on **P1**, **P2**, and PDHBT were fabricated from chlorobenzene. All the FET devices were fabricated by employing a top-contact configuration for reducing the contact resistance. Figure 8 shows the FET transfer curves and output characteristics of the copolymer devices on the ODTs-modified SiO₂. In the saturation region ($V_d > V_g - V_t$), I_d can be described by the equation⁴⁰

$$I_{ds} = \frac{WC_0\mu}{2L}(V_g - V_t)^2$$

where W and L are the channel width and length, respectively, C_0 is the capacitance of the gate insulator per unit area (SiO₂, 300 nm, $C_0 = 10$ nF/cm²), μ is the hole mobility, and V_t is the threshold voltage. The saturation-regime mobility was estimated from the slope of the plot of the drain-to-source current (I_d)^{1/2} as a function of the gate voltage (V_g). FET devices based on the polymer films were processed with and without annealing at 100 °C. The corresponding carrier mobilities are listed in Table 3, and the typical p-type transfer and output characteristics of the studied polymers are shown in Figure 8 and Figure S6. The average FET hole mobility (μ) value of **P1** was determined to be 1.66×10^{-4} cm² V⁻¹ s⁻¹ without annealing and increased to 1.41×10^{-3} cm² V⁻¹ s⁻¹ after annealing with the high ON/OFF ratio of 7.8×10^5 . In contrast, **P2** shows much higher average μ values of 4.82×10^{-2} cm² V⁻¹ s⁻¹ (without annealing) and 8.81×10^{-2} cm² V⁻¹ s⁻¹ (after annealing) than **P1**, with an adequate ON/OFF ratio. For comparison, PDHBT without the electron-accepting OXD or TD moiety shows a μ value of 2.10×10^{-4} cm² V⁻¹ s⁻¹ after annealing (Figure S6), which is in good agreement with the value in the literature³³ and is lower than that of either **P1** or **P2**. This result indicated that the incorporation of the electron-acceptor moieties efficiently enhances the charge transport due to the D–A intramolecular charge transfer as well as the compact packing structure, as demonstrated by the GIXD characteristics. In addition, all the studied polymers showed

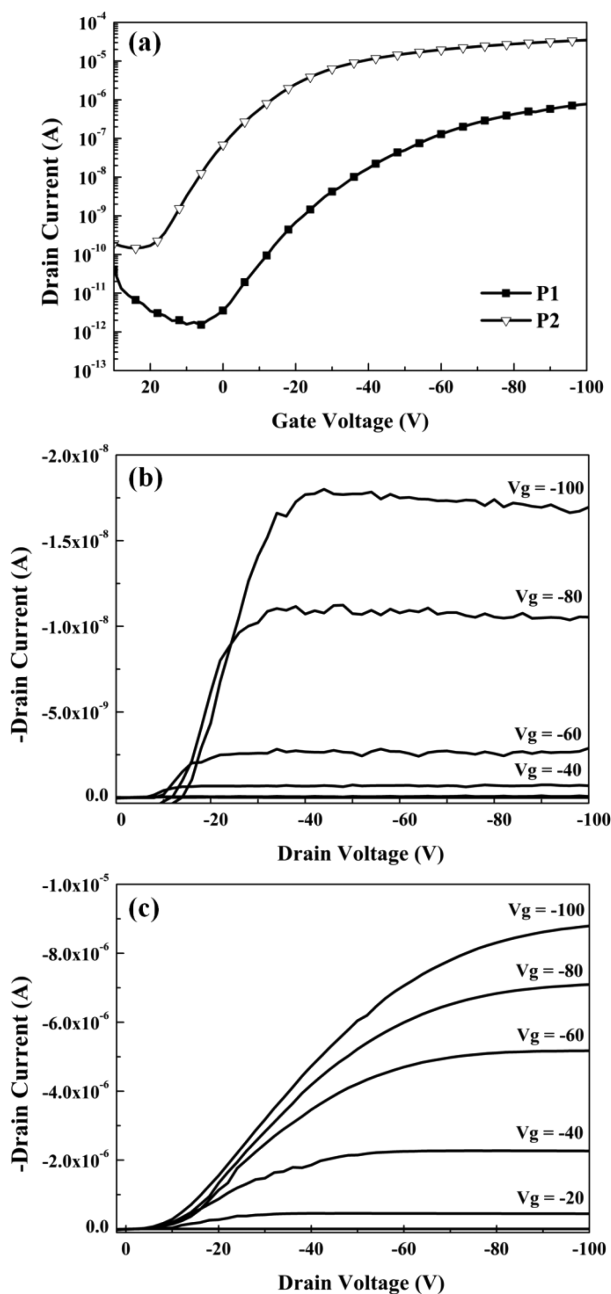


Figure 8. (a) The p-type FET transfer characteristics of **P1** and **P2** thin films and the p-type output characteristics of (b) **P1** and (c) **P2**.

Table 3. Field-effect Transistor Characteristics of **P1**, **P2**, and PDHBT^a

polymer	annealing temp (°C)	hole mobility ^{avg} (cm ² V ⁻¹ s ⁻¹)	ON/OFF ^{avg}	V_t (V)
P1	non	1.66×10^{-4}	4.0×10^4	-38
P1	100	1.41×10^{-3}	7.8×10^5	-32
P2	non	4.81×10^{-2}	2.3×10^6	-4.1
P2	100	8.81×10^{-2} (max: 0.12)	5.3×10^5	2.1
PDHBT	non	8.86×10^{-5}	1.3×10^4	2.1
PDHBT	100	2.10×10^{-4}	7.0×10^3	9.8

^aChlorobenzene was used as solvent for casting the polymers.

higher mobility after thermal annealing because of the molecular packing was enhanced as evidenced by GIXD results.

In particular, the maximum mobility of **P2** after annealing reached $0.12 \text{ cm}^2 \text{ V}^{-1} \text{ s}^{-1}$ (average: $8.81 \times 10^{-2} \text{ cm}^2 \text{ V}^{-1} \text{ s}^{-1}$), which is comparable to that of **P3HT**. These results are correlated with the more crystalline and ordered nanofibrillar morphology of **P2** than either **P1** or **PDHBT**, as previously described. The high threshold voltage of **P1** probably comes from its very low HOMO energy levels (-5.55 eV), leading to a high energy barrier for hole injection.

Polymer Solar Cell Characteristics. The structure of ITO/PEDOT:PSS (30 nm)/polymer:PCBM (1:1, w/w)/Ca (30 nm)/Al (100 nm) was fabricated for the PSC characterization under the AM 1.5 G illumination condition (100 mW cm^{-2}). The active layers of the studied devices were prepared through nonannealing or thermal annealing at $100 \text{ }^\circ\text{C}$ for 10 min. The J - V curves of the polymer/PCBM BHJ PSC devices were measured under an ambient condition after encapsulating them using glass covers and UV-curing glue, as shown in Figure 9. The PSC characteristics, including the open-circuit voltage

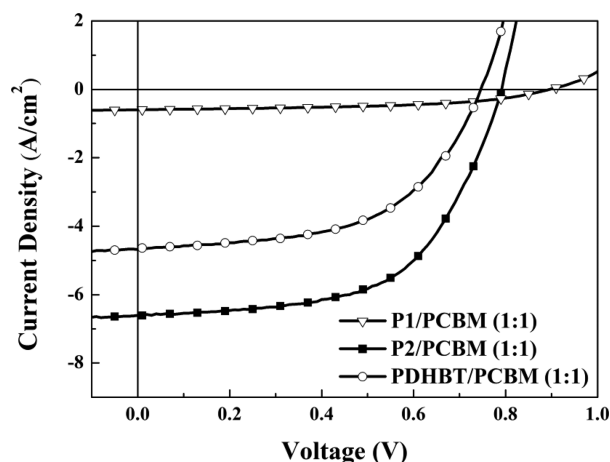


Figure 9. J - V curves of the PSCs based on polymer/PCBM (1:1, w/w) under the illumination of AM 1.5, 100 mW/m^2 .

(V_{oc}), short-circuit current density (J_{sc}), fill factor (FF), and power conversion efficiency (PCE), of the **P1**, **P2**, and **PDHBT** devices are summarized in Table 4.

Table 4. Photovoltaic Cell Characteristics of Polymer/PCBM (1:1, w/w) under the Illumination of AM 1.5, 100 mW/m^2

polymers	annealing temp ($^\circ\text{C}$)	V_{oc} (V)	J_{sc} (mA/cm^2)	FF	PCE ^a (%)
P1	non	0.81	0.713	0.498	0.284
P1	100 $^\circ\text{C}$, 10 min	0.90	0.599	0.515	0.277
P2	non	0.80	6.60	0.576	3.04
P2	100 $^\circ\text{C}$, 10 min	0.86	4.57	0.522	2.05
PDHBT	non	0.75	4.67	0.546	1.91
PDHBT	100 $^\circ\text{C}$, 10 min	0.78	4.36	0.473	1.61

^aThe average value of PCE was calculated from 4 pixels in the device.

For **P1**, the high V_{oc} values (0.81–0.90 V) are attributed to their low HOMO energy levels; however, the J_{sc} values are very low at less than 1 mA/cm^2 , resulting in the low PCE of 0.28%. This is because **P1** inefficiently absorbs light and its hole mobility is lower than **P2**, derived from less ordered packing structures that prevents separated charge generation and smooth charge transportation. Unfortunately, changing the

film thickness as well as the annealing process does not improve PCE.

In a sharp contrast, **P2** shows much improved J_{sc} values of 4.57 – 6.60 mA/cm^2 , while maintaining the high V_{oc} values (0.80–0.86 V) due to efficient light harvesting, high hole mobility, and low HOMO energy levels. As a result, the highest PCE (3.04%) could be achieved with a V_{oc} value of 0.80 V, a J_{sc} value of 6.60 mA/cm^2 , and a FF value of 0.576 after optimization of the solvent and spin rate for casting the polymers (see Figure 9). It should be mentioned that the value of 0.80 V of V_{oc} and the value of 6.60 mA/cm^2 of J_{sc} of **P2** are higher than those of the **PDHBT**:PCBM BHJ PSC devices due to its low-lying HOMO levels and high field-effect hole mobility, leading to a higher PCE for **P2** (3.04%) than for **PDHBT** (1.91%). These results demonstrate that the incorporation of the TD acceptor units into the thiophene-based polymer main chain lowers the HOMO energy levels as well as enhances the charge transporting to achieve a high PCE of the devices. Furthermore, the PCE of over 3% is the first observation using TD-incorporated π -conjugated polymers in PSC applications. However, the annealing process decreases the PCE of **P2**, even though the hole mobility increases after annealing as previously described. There is no clear explanation for this result at the present time, but the morphological change, such as aggregation, might occur after annealing, which generally causes a reduction in the interface areas of the p-type and n-type domains to limit the charge separation.

Figure 10 shows the photocurrent action spectra of the ITO/PEDOT:PSS (30 nm)/polymer:PCBM (1:1, w/w)/Ca (30

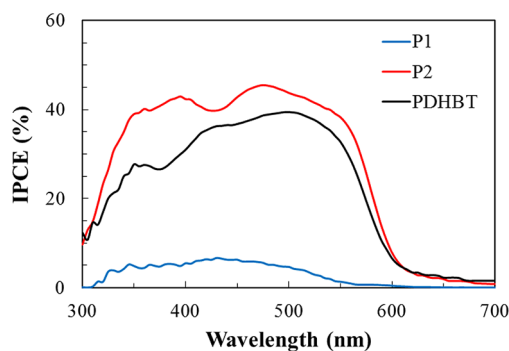


Figure 10. Photocurrent action spectrum of the devices based on (a) **P1**/PCBM (1:1, w/w), (b) **P2**/PCBM (1:1, w/w), and (c) **PDHBT**/PCBM (1:1, w/w).

nm)/Al (100 nm) devices, in which **P1**, **P2**, and **PDHBT** (reference) are compared. All the devices exhibited a relatively broad photoresponse between 300 and 620 nm (300–550 nm for **P1**), indicating that the absorption of the polymer:PCBM blends reflects the photocurrents in these wavelength regions. The device based on **P1** shows a significantly low maximum incident photon-to-current conversion efficiency (IPCE) value of 7%, which is coincident with the very low J_{sc} value for the photovoltaic performance of the **P1**:PCBM PSC device, as mentioned above. In contrast, the device based on **P2** exhibits the highest maximum IPCE value of 46% among the three devices. Such a high photoconversion efficiency agrees well with the highest J_{sc} and PCE values of the **P2**:PCBM PSC device.

CONCLUSIONS

We have successfully synthesized newly designed polythiophene derivatives bearing OXD or TD units, **P1** and **P2**, by the Stille coupling reaction. The FET and PSC characteristics of **P1** and **P2** were investigated to determine the hole mobility and PCE, respectively. The higher mobility of **P2** than that of **P1** was related to its orderly nanofibrillar structure. The PSC based on **P2**:PCBM = 1:1 (w/w) reached a PCE of 3.04% with the J_{sc} value of 6.60 mA/cm², the V_{oc} value of 0.80 V, and the FF value of 0.576, under the illumination of AM 1.5, 100 mW/cm². It also showed the maximum IPCE value of 46%. The highest PCE (3.04%) value among the TD-based polymers ever reported may be attributed to the high hole mobility of **P2** (8.81×10^{-2} cm² V⁻¹ s⁻¹). In addition, the introduction of TD units significantly affects lowering of the HOMO energy levels, resulting in the achievement of high V_{oc} and PCE values without sacrificing light harvesting.

ASSOCIATED CONTENT

Supporting Information

SEC and TGA curves, ESP surfaces and 2D GIXD patterns of **P1**, **P2**, and PDHBT, tapping mode AFM phase images of **P1** and **P2**, and FET transfer curves and output characteristics of PDHBT films (Figures S1–S6). This material is available free of charge via the Internet at <http://pubs.acs.org>.

AUTHOR INFORMATION

Corresponding Author

*E-mail: thigashihara@polymer.titech.ac.jp (T.H.); chenwc@ntu.edu.tw (W.-C.C.).

Author Contributions

[†]Hung-Chin Wu and Tetsunari Mizobe equally contributed to this work.

Notes

The authors declare no competing financial interest.

ACKNOWLEDGMENTS

The financial support of this work from Japan Science and Technology Agency (JST), PRESTO program and National Science Council, and the Excellence Research Program of National Taiwan University is highly appreciated. W.-C. Chen also acknowledges the helpful discussions on the GIXD experiment with Prof. Ya-Sen Sun at National Central University of Taiwan.

REFERENCES

- (1) Yu, G.; Gao, J.; Hummelen, J. C.; Wudl, F.; Heeger, A. J. *Science* **1995**, *270*, 1789.
- (2) Cheng, Y. J.; Yang, S. H.; Hsu, C. S. *Chem. Rev.* **2009**, *109*, 5868.
- (3) Peet, J.; Kim, J. Y.; Coates, N. E.; Ma, W. L.; Moses, D.; Heeger, A. J.; Bazan, G. C. *Nat. Mater.* **2007**, *6*, 497.
- (4) Tsai, J. H.; Chueh, C. C.; Lai, M. H.; Wang, C. F.; Chen, W. C.; Ko, B. T.; Ting, C. *Macromolecules* **2009**, *42*, 1897.
- (5) Peet, J.; Heeger, A. J.; Bazan, G. C. *Acc. Chem. Res.* **2009**, *42*, 1700.
- (6) Li, G.; Shrotriya, V.; Huang, J. S.; Yao, Y.; Moriarty, T.; Emery, K.; Yang, Y. *Nat. Mater.* **2005**, *4*, 864.
- (7) Yang, X. N.; Loos, J.; Veenstra, S. C.; Verhees, W. J. H.; Wienk, M. M.; Kroon, J. M.; Michels, M. A. J.; Janssen, R. A. J. *Nano Lett.* **2005**, *5*, 579.
- (8) Chueh, C. C.; Higashihara, T.; Tsai, J. H.; Ueda, M.; Chen, W. C. *Org. Electron.* **2009**, *10*, 1541.
- (9) Blouin, N.; Michaud, A.; Leclerc, M. *Adv. Mater.* **2007**, *19*, 2295.
- (10) Kim, Y.; Cook, S.; Tuladhar, S. M.; Choulis, S. A.; Nelson, J.; Durrant, J. R.; Bradley, D. D. C.; Giles, M.; McCulloch, I.; Ha, C. S.; Ree, M. *Nat. Mater.* **2006**, *5*, 197.
- (11) Li, Y. F.; Zou, Y. P. *Adv. Mater.* **2008**, *20*, 2952.
- (12) Chang, Y. T.; Hsu, S. L.; Chen, G. Y.; Su, M. H.; Singh, T. A.; Diao, E. W. G.; Wei, K. H. *Adv. Funct. Mater.* **2008**, *18*, 2356.
- (13) Xin, H.; Kim, F. S.; Jenekhe, S. A. *J. Am. Chem. Soc.* **2008**, *130*, 5424.
- (14) Liang, Y. Y.; Wu, Y.; Feng, D. Q.; Tsai, S. T.; Son, H. J.; Li, G.; Yu, L. P. *J. Am. Chem. Soc.* **2009**, *131*, 56.
- (15) Hou, J. H.; Tan, Z. A.; Yan, Y.; He, Y. J.; Yang, C. H.; Li, Y. F. *J. Am. Chem. Soc.* **2006**, *128*, 4911.
- (16) Scharber, M. C.; Mühlbacher, D.; Koppe, M.; Denk, P.; Waldauf, C.; Heeger, A. J.; Brabec, C. J. *Adv. Mater.* **2006**, *18*, 789.
- (17) Liang, Y.; Xu, Z.; Xia, J.; Tsai, S.-T.; Wu, Y.; Li, G.; Ray, C.; Yu, L. *Adv. Mater.* **2010**, *22*, E135.
- (18) Chu, T.-Y.; Lu, J.; Beaupré, S.; Zhang, Y.; Pouliot, J.-R.; Wakim, S.; Zhou, J.; Leclerc, M.; Li, Z.; Ding, J.; Tao, Y. *J. Am. Chem. Soc.* **2011**, *133*, 4250.
- (19) Zhou, H.; Yang, L.; Stuart, A. C.; Price, S. C.; Liu, S.; You, W. *Angew. Chem., Int. Ed.* **2011**, *50*, 2995.
- (20) Amb, C. M.; Chen, S.; Graham, K. R.; Subbiah, J.; Small, C. E.; So, F.; Reynolds, J. R. *J. Am. Chem. Soc.* **2011**, *133*, 10062.
- (21) He, Z.; Zhong, C.; Huang, X.; Wong, W.-Y.; Wu, H.; Chen, L.; Su, S.; Cao, Y. *Adv. Mater.* **2011**, *23*, 4636.
- (22) Service, R. F. *Science* **2011**, *332*, 293.
- (23) Mühlbacher, D.; Scharber, M.; Morana, M.; Zhu, Z.; Waller, D.; Gaudiana, R.; Brabec, C. *Adv. Mater.* **2006**, *18*, 2884.
- (24) Coffin, R. C.; Peet, J.; Rogers, J.; Bazan, G. C. *Nat. Chem.* **2009**, *1*, 657.
- (25) Park, S. H.; Roy, A.; Beaupré, S.; Cho, S.; Coates, N.; Moon, J. S.; Moses, D.; Leclerc, M.; Lee, K.; Heeger, A. J. *Nat. Photonics* **2009**, *3*, 297.
- (26) Ong, K.-H.; Lim, S.-L.; Tan, H.-S.; Wong, H.-K.; Li, J.; Ma, Z.; Moh, L. C. H.; Lim, S.-H.; de Mello, J. C.; Chen, Z.-K. *Adv. Mater.* **2011**, *23*, 1409.
- (27) Zhang, M.; Guo, X.; Wang, X.; Wang, H.; Li, Y. *Chem. Mater.* **2011**, *23*, 4264.
- (28) Du, C.; Li, C.; Li, W.; Chen, X.; Bo, Z.; Veit, C.; Ma, Z.; Wuerfel, U.; Zhu, H.; Hu, W.; Zhang, F. *Macromolecules* **2011**, *44*, 7617.
- (29) Umeyama, T.; Douvogianni, E.; Imahori, H. *Chem. Lett.* **2012**, *41*, 354.
- (30) Patil, P. S.; Haram, N. S.; Pal, R. R.; Periasamy, N.; Wadgaonkar, P. P.; Salunkhe, M. M. *J. Appl. Polym. Sci.* **2012**, *125*, 1882.
- (31) Tkachov, R.; Senkovskyy, V.; Komber, H.; Kiriy, A. *Macromolecules* **2011**, *44*, 2006.
- (32) Zhou, W.; Shen, P.; Zhao, B.; Jiang, P.; Deng, L.; Tan, S. *J. Polym. Sci., Part A: Polym. Chem.* **2011**, *49*, 2685.
- (33) Ko, S.; Hoke, E. T.; Pandey, L.; Hong, S.; Mondal, R.; Risko, C.; Yi, Y.; Noriega, R.; McGehee, M. D.; Bredas, J.-L.; Salbeck, J.; Bao, Z. *J. Am. Chem. Soc.* **2012**, *134*, 5222.
- (34) Frisch, M. J.; Trucks, G. W.; Schlegel, H. B.; Scuseria, G. E.; Robb, M. A.; Cheeseman, J. R.; Montgomery, J. A., Jr.; Vreven, T.; Kudin, K. N.; Burant, J. C.; Millam, J. M.; Iyengar, S. S.; Tomasi, J.; Barone, V.; Mennucci, B.; Cossi, M.; Scalmani, G.; Rega, N.; Petersson, G. A.; Nakatsuji, H.; Hada, M.; Ehara, M.; Toyota, K.; Fukuda, R.; Hasegawa, J.; Ishida, M.; Nakajima, T.; Honda, Y.; Kitao, O.; Nakai, H.; Klene, M.; Li, X.; Knox, J. E.; Hratchian, H. P.; Cross, J. B.; Bakken, V.; Adamo, C.; Jaramillo, J.; Gomperts, R.; Stratmann, R. E.; Yazyev, O.; Austin, A. J.; Cammi, R.; Pomelli, C.; Ochterski, J. W.; Ayala, P. Y.; Morokuma, K.; Voth, G. A.; Salvador, P.; Dannenberg, J. J.; Zakrzewski, V. G.; Dapprich, S.; Daniels, A. D.; Strain, M. C.; Farkas, O.; Malick, D. K.; Rabuck, A. D.; Raghavachari, K.; Foresman, J. B.; Ortiz, J. V.; Cui, Q.; Baboul, A. G.; Clifford, S.; Cioslowski, J.; Stefanov, B. B.; Liu, G.; Liashenko, A.; Piskorz, P.; Komaromi, I.; Martin, R. L.; Fox, D. J.; Keith, T.; Al-Laham, M. A.; Peng, C. Y.; Nanayakkara, A.; Challacombe, M.; Gill, P. M. W.; Johnson, B.; Chen,

W.; Wong, M. W.; Gonzalez, C.; Pople, J. A. *Gaussian 03, revision B.04*; Gaussian, Inc.: Wallingford, CT, 2004.

(35) Yu, C. Y.; Chen, C. P.; Chan, S. H.; Hwang, G. W.; Ting, C. *Chem. Mater.* **2009**, *21*, 3262.

(36) Salzner, U.; Lagowski, J. B.; Pickup, P. G.; Poirier, R. A. *Synth. Met.* **1998**, *96*, 177.

(37) Bredas, J. L.; Silbey, R.; Boudreaux, D. S.; Chance, R. R. *J. Am. Chem. Soc.* **1983**, *105*, 6555.

(38) Yang, H. C.; Shin, T. J.; Yang, L.; Cho, K.; Ryu, C. Y.; Bao, Z. N. *Adv. Funct. Mater.* **2005**, *15*, 671.

(39) Lu, C.; Wu, H. C.; Chiu, Y. C.; Lee, W. Y.; Chen, W. C. *Macromolecules* **2012**, *45*, 3047.

(40) Zaumseil, J.; Friend, R. H.; Sirringhaus, H. *Nat. Mater.* **2005**, *5*, 69.